Anti-regression on manifolds with an application to 3D projective shape analysis

Y. Deng, V. Patrangenaru and V. Balan

Abstract. Given a *random object* X on a compact metric space $\mathcal{M}$, provided with a "chord" distance induced by the Euclidean distance on the numerical space where $\mathcal{M}$ is embedded, one considers the *Fréchet function*, expected square of the chord distance from the random object X to a point on $\mathcal{M}$. This function attains its maximum at a set of points, called the *extrinsic antimean set*. In case the extrinsic antimean set has one point only, that point is called *extrinsic antimean* of X. Given a pair of random objects (Y, X) on a product of object spaces $\mathcal{N} \times \mathcal{M}$, where $\mathcal{M}$ is compact and is embedded into a numerical space, the value of the *anti-regression function* at a point y on $\mathcal{N}$ as the conditional extrinsic antimean of X given $Y = y$. Here one gives necessary and sufficient conditions that insure that the antiregression function is well defined, and as an application one gives an example of extrinsic anti-regression in projective shape analysis for a clamshells species found in the Florida panhandle, where the predictor is age and the response is $3D$ projective shape.

M.S.C. 2010: 62G08, 62H35.
Key words: projective shape; VW-embedding; nonparametric anti-regression; antimeans.

1 Introduction

In Statistics an *object* is a certain type of feature extracted from raw data, such as a shape, a direction, a color, etc., that can be represented as a point in a complete metric space $(\mathcal{M}, \rho)$, called *object space.* Important examples of objects are direct similarity shapes of configurations extracted from digital camera images, or from medical imaging outputs. For such data, the associated objects can be represented as points in Kendall shape spaces (see [4]), in affine shape spaces (see [10]), or in projective shape spaces (see [9]). Other examples of object spaces are axial spaces, or spaces of directions (see [5]), or spaces of perceived colors (see [13]). As an example of an object from a digital camera image, one may extract the projective shape of a

BSG Proceedings, vol. 25, 2018, pp. 34-44.
© Balkan Society of Geometers, Geometry Balkan Press 2018.

list of 2D pixel coordinates of a group five labeled points drawn on a white board; this is a 2D projective shape of a pentad.

Therefore a *random object* X can be thought of as a random point in a complete metric space $(\mathcal{M}, \rho)$. Formally, if $\mathcal{B}_\rho$ is the Borel σ-algebra generated by open sets of $(\mathcal{M}, \rho)$, and $(\Omega, \mathcal{A}, \mathbb{P})$ is a probability space, then a random object is a function $X : \Omega \to M$, such that for all $B \in \mathcal{B}_\rho$, $X^{-1}(B)$ is in $\mathcal{A}$. For example a random projective shape of a pentad in general position is a random point of the projective shape space $P\Sigma_2^5$, and in case the pentad contains a projective frame at four given landmark locations, the associated random projective shape can be regarded as a random point in $\mathbb{R}P^2$ (see [7]).

In general, if one considers an object space $\mathcal{M}$ provided with a "chord" distance ρ_j associated to an embedding $j : \mathcal{M} \to \mathbb{R}^N$, $\rho_j(p_1, p_2) = \|j(p_1) - j(p_2)\|$, the statistical analysis performed relative to the distance ρ_j is termed *extrinsic data analysis*. The expected square distance from the random object X to an arbitrary point p defines the *Fréchet function* associated with X, given by $\mathcal{F}_j(p) = E\|j(X) - j(p)\|^2$.

The examples of object spaces mentioned above are all *compact spaces*, therefore in Section 2 we introduce the *extrinsic antimean set* as set of maximizers of the Fréchet function. In case the extrinsic antimean set has one point only, that point is called *extrinsic antimean* of X, and is labeled $\alpha E_j(X)$. Necessary and sufficient conditions for the existence of the extrinsic antimean are also given in this section. In Section 3, given a pair (Y, X) of random objects on a product of object spaces $\mathcal{N} \times \mathcal{M}$, where $\mathcal{M}$ is compact, and j is an embedding of $\mathcal{M}$ into an Euclidean space, the *anti-regression function* $\alpha F : \mathcal{N} \to \mathcal{M}$ is defined by the conditional extrinsic antimean formula $\alpha F(x) = \alpha E_j(Y|X = x)$. In this section we also give a sample anti-regression function estimator, in case the predictor is a numerical covariate. This estimator involves a kernel smoothing function, that is applied to the numerical predictor. In Section 4, we consider some general preliminaries on projective shape analysis, that are necessary in our data analysis; concepts of projective transformations, projective shapes and projective coordinates relative to a given projective frame are considered here. In Section 5, the reader is introduced to the methodology of 3D projective shape data collection from digital camera images, using a powerful image reconstruction software, that can recover the 3D surface of a scene from its digital images, via color correlation at matched configurations. The landmark configuration, and projective its projective shape, that are used our data analysis are also described here. In Section 6, we run the anti-regression analysis for 3D projective shapes, via a Veronese-Whitney (VW) embedding of the projective shape space of finite configurations of projective shapes including a projective frame at the first five landmark locations. The paper concludes with a short discussion.

2 Fréchet functions and extrinsic antimeans

Fréchet [3] noticed that for nonlinear data, numbers or vectors are not giving a meaningful description. To investigate these kind of data he came up with a notion of "elements", which are nowadays called *objects*. In his paper [3], as example of an object, he mentioned the shape of an egg randomly taken from a basket of eggs; object data analysis has arisen in areas such as analysis of shapes of configurations extracted from digital images, or from medical imaging outputs. To analyse the mean

and variance of a random object X, Fréchet defined what we call today the *Fréchet function,* as follows:

$$\mathcal{F}(p) = \mathbb{E}(\rho^2(p, X)). \tag{2.1}$$

Its minimizers form the *Fréchet mean set*. In case when ρ is the "chord" distance on $\mathcal{M}$ induced by the Euclidean distance in $\mathbb{R}^N$ via an embedding $j : \mathcal{M} \to \mathbb{R}^N$, the Fréchet function becomes

$$\mathcal{F}(p) = \int_{\mathcal{M}} \|j(x) - j(p)\|^2 Q(dx), \tag{2.2}$$

where $Q = P_X$ is the probability measure on $\mathcal{M}$, associated with X, and $\|\cdot\|$ is the Euclidean norm. In this case, since we use an embedding, the Fréchet mean set is called the *extrinsic mean set* (see [**?**]), and if we have a unique point in the extrinsic mean set of X, this point is called the *extrinsic mean* of X, and is labeled $\mu_E(X)$ or simply μ_E. Also, given $X_1, \ldots, X_n$ independent identically distributed random objects (i.i.d.r.o.'s) from Q, their *extrinsic sample mean (set)* is the extrinsic mean (set) of the empirical distribution $\hat{Q}_n = \frac{1}{n}\sum_{i=1}^n \delta_{X_i}$.

In this paper we assume that $(\mathcal{M}, \rho)$ is a compact metric space, therefore the Fréchet function is bounded, and its extreme values are attained at points on $\mathcal{M}$. We are introducing a *new location parameter* for X, following a definition from [7].

Definition 2.1. The set of maximizers of the Fréchet function is called the *extrinsic antimean set*. In case the extrinsic antimean set has one point only, that point is called *extrinsic antimean* of X, and is labeled $\alpha\mu_{j,E}(Q)$, or simply $\alpha\mu_E$, when j is known.

Definition 2.2. A point $y \in \mathbb{R}^N$for which there is a unique point $p \in \mathcal{M}$ satisfying the equality

$$\sup_{x\in\mathcal{M}} ||y - j(x)|| = \|y - j(p)\| \tag{2.3}$$

is called αj-nonfocal. A point which is not αj-nonfocal is said to be αj-focal. If y is an αj-nonfocal point, its farthest projection on $j(\mathcal{M})$ is the unique point $z = P_{F,j}(y) \in j(\mathcal{M})$ with $\sup_{x\in\mathcal{M}} ||y - j(x)|| = \|y - z\|$.

Definition 2.3. A probability distribution Q on $\mathcal{M}$ is said to be αj-nonfocal if the mean μ of $j(Q)$ is αj-nonfocal.

The following is a description of the antimean

Theorem 2.1. *([11]) Let μ be the mean vector of $j(Q)$, then the following hold true:*

1. *The extrinsic antimean set is the set of all points $p \in \mathcal{M}$ such that $\sup_{x\in\mathcal{M}} ||\mu - j(x)|| = \|\mu - j(p)\|$.*
2. *If $\alpha\mu_{j,E}(Q)$ exists, then μ is αj-nonfocal and $\alpha\mu_{j,E}(Q) = j^{-1}(P_{F,j}(\mu))$.*

The consistency of the sample antimean is given below:

Theorem 2.2. *([12]) Let $Q = P_X$ be a probability measure associated with the random object X on a compact metric space $(\mathcal{M}, d)$. Assume $F(p) = E(d^2(p, X))$ is finite on $\mathcal{M}$. Then (a) given any $\varepsilon > 0$, there exist a P-null set N, such that $\forall\, \omega \in N^c$, there is an $n(\omega) < \infty$ such that the Fréchet (sample) antimean set of $\hat{Q}_n = \hat{Q}_{n,\omega}$ is contained in the ε-neighborhood of the Fréchet antimean set of Q for all $n \geq n(\omega)$. (b) If the Fréchet antimean of Q exists, then every measurable choice from the Fréchet (sample) antimean set of $\hat{Q}_n$ is a strongly consistent estimator of the Fréchet antimean of Q.*

3 Anti-regression function with c covariates and response on a manifold

We assume that the response variable Y takes values on $(\mathcal{M}, \rho)$, a compact metric space embedded via j in $\mathbb{R}^N$, and the predictor X takes values in $\mathcal{N}$. The goal is to build an anti-regression function between Y and X. Let us assume for simplicity that given a pair of objects (X, Y), f_X is the marginal density of X w.r.t. a fixed measure ν on $\mathcal{N}$ and $f_Y(\cdot|x)$ is the conditional density function of Y given X, relative to a fixed measure λ on $\mathcal{M}$ (in case M is a homogeneous space, one may assume in addition that λ is invariant w.r.t. a transitive group action on $\mathcal{M}$). We define the *anti-regression function* $\alpha F(x)$ as

$$\alpha F(x) = \arg\max_{q \in \mathcal{M}} \int_{\mathcal{M}} \rho^2(q, y) P(\, dy|x). \tag{3.1}$$

Using Theorem 2.1, we first calculate the mean of the conditional distribution $P(Y|x)$, to which we apply the farthest projection $P_{F,j}$ mentioned in Definition 2.2. The anti-regression function becomes:

$$\alpha F(x) = j^{-1} \circ P_{F,j} \circ \int_{j(\mathcal{M})} z \tilde{P}(\, dz|x), \tag{3.2}$$

where $\tilde{P}(\cdot|x) = P(\cdot|x) \circ j^{-1}$ is the conditional probability measure on $j(\mathcal{M})$ induced by the conditional probability measure $P(\cdot|x)$ via the embedding j.

Now we give an estimator for $\alpha F(x)$. Assume we have the observations $(x_i, y_i), i = 1, \ldots, n$ where the predictor is a *vector of covariates* $X = (X^1, \ldots,\ X^c)^T$. Let$K : \mathbb{R}^c \to \mathbb{R}$ be a multivariate kernel function such that $\int_{\mathbb{R}^c} K(x)\, dx = 1$ and $\int_{\mathbb{R}^c} xK(x)\, dx = 0$. One can take K to be a product of c one-dimensional kernel functions. For example, let H be the

$$H = diag(h_1, \ldots, h_k), \tag{3.3}$$

with $h_i > 0 (i = 1, \ldots, c)$ be the bandwidth matrix and $|H| = h_1 \ldots h_k$. Let $K_H(x) = \frac{1}{|H|} K(H^{-1}x)$ and

$$\hat{F}(x) = \sum_{i=1}^{n} \frac{K_H(x_i - x)}{\sum_{i=1}^{n} K_H(x_i - x)} j(y_i). \tag{3.4}$$

This is the proposed estimator of $\int_{j(\mathcal{M})} z\tilde{P}(\,dz|x)$ which is generally the weighted mean of $j(y_i), i = 1, \ldots, n$ with weight h_r. Now we can define the extrinsic kernel estimator of the anti-regression function $\alpha F(x)$ as

$$\widehat{\alpha F(x)} = j^{-1} \circ P_{F,j} \circ \hat{F}(x) = j^{-1}(\arg\max_{q \in \mathcal{M}} ||q - \hat{F}(x)||). \tag{3.5}$$

To apply the anti-regression model, we separate the procedure into two parts. First we need to calculate $\int_{j(\mathcal{M})} z\tilde{P}(\,dz|x)$, which can be estimated by formula (3.4). Secondly we project $\hat{F}(x)$ to a point on $j(\mathcal{M})$ which is the farthest point from $\hat{F}(x)$, and apply the inverse of the embedding j.

4 Projective shape space of 3D configurations

Since our anti-regression analysis will have a 3D projective shape response, some preliminaries about projective shapes are necessary.

4.1 Projective frames and projective shapes in $\mathbb{R}P^m$

We will use the notation $[x]$ to represent an element of $\mathbb{R}P^m$, with $x \in \mathbb{R}^{m+1}\backslash\{0\}$. The equivalence class of $x = (x^1, \ldots, x^{m+1})$, where two vectors x, x' are equivalent if they differ by a nonzero multiple, is also denoted as $[x^1 : x^2 : \cdots : x^{m+1}]$, featuring the *homogeneous coordinates* $(x^1, \ldots, x^{m+1})$ of $[x]$, which are unique up to a nonzero multiplicative constant.

Definition 4.1. A projective transformation α_A of $\mathbb{R}P^m$ associated with a nonsingular matrix $A \in GL(m+1, \mathbb{R})$ has the form

$$\alpha_A([x^1 : \cdots : x^{m+1}]) = [A(x^1, \ldots, x^{m+1})^T]. \tag{4.1}$$

This is a well defined map, since if one multiplies the matrix A by a nonzero constant, then the right hand side of (4.3) does not change. Projective transformations form the group $PGL(m)$ of projective transformations of $\mathbb{R}P^m$, which has a Lie group structure of dimension $(m+1)^2-1 = m(m+2)$. Note that a projective transformation is determined by its values on $m+2$ points in general position, leading to the following:

Definition 4.2. The *projective frame* in $\mathbb{R}P^m$ is an ordered set of $m+2$ projective points in general position.

An example of projective frame in $\mathbb{R}P^m$ is the *standard projective frame*

$$([e_1], \ldots, [e_{m+1}], [e_1 + ... + e_{m+1}]).$$

In projective shape analysis it is preferable to employ coordinates invariant with respect to the group $PGL(m)$. A projective transformation takes a projective frame to a projective frame, and its action on $\mathbb{R}P^m$ is determined by its action on a projective frame. Therefore, if we define the *projective coordinate(s)* of a point $p \in \mathbb{R}P^m$ w.r.t. a projective frame $\pi = (p_1, \ldots, p_{m+2})$ as being given by

$$p^\pi = \beta^{-1}(p), \tag{4.2}$$

where $\beta \in PGL(m)$ is a projective transformation taking the standard projective frame to π, these coordinates have automatically the invariance property. A *k-ad* is a set of k labeled points in $(\mathbb{R}P^m)^k$; a k-ad can be regarded as a point on $(\mathbb{R}P^m)^k$.

Definition 4.3. A *projective shape* of a k-ad is the orbit of that k-ad under the diagonal action of $PGL(m)$ on $(\mathbb{R}P^m)^k$ given by

$$\alpha_k(\alpha_A, (p_1, ..., p_k)) = (\alpha_A(p_1), ..., \alpha_A(p_k))$$

The m-dimensional projective shape of a *generic k-ad* is determined by the *projective coordinates* $(p^\pi_{m+3}, ..., p^\pi_k)$ of $k - m - 2$ of its points, relative to the remaining $(m + 2)$ of its points that form a projective frame, which for convenience are selected here to be the first points in the k-ad. Thus the set $P\Sigma^k_m$ of projective shapes of generic k-ads including a projective frame at given labels, is isomorphic to $(\mathbb{R}P^m)^{k-m-2}$ [9]. This representation is dependent on the choice of the projective frame, however a representation of projective shapes of generic k-ads, that is independent of the projective frame selection, that can be obtained as well, does not improve significantly the analysis. The manifold structure of this space allows using the *asymptotic theory for means and antimeans on manifolds*.

Furthermore, for $m = 3$, this projective shape space has in addition a Lie group structure, which is helpful when dealing with pairs of data (see Crane and Patrangenaru (2011)[2]).

For each 3D object in our data, we focus on the 3D coordinates of a certain configuration of k labeled landmarks. We say that two such configurations of labeled points in $\mathbb{R}^3$ have *the same projective shape* if they differ by a *projective transformation* of $\mathbb{R}^3$.

Note that while a projective transformation ν of $\mathbb{R}^m$ is defined in terms of a matrix $A = (a^j_i) \in GL(m + 1, \mathbb{R})$, via $\nu((x^1, \ldots, x^m)) = (y^1, \ldots, y^m)$,

$$y^j = \frac{\sum_{i=1}^m a^j_i x^i + a^j_{m+1}}{\sum_{i=1}^m a^{m+1}_i x^i + a^{m+1}_{m+1}}, \ \forall j = 1, \ldots, m, \tag{4.3}$$

in applications it is easier to identify $\mathbb{R}^m$ with an open affine subset of $\mathbb{R}P^m$, and consequently rather than looking at a k-ad in $\mathbb{R}^m$ one may consider the corresponding k-ad in $\mathbb{R}P^m$, and extending the pseudo-action by the projective transformations on open dense subsets of $\mathbb{R}^m$ to a group action of the projective group $PGL(m)$ on $\mathbb{R}P^m$, $\alpha : \ PGL(m) \times \mathbb{R}P^m \to \mathbb{R}P^m$, where

$$\alpha([A], [x]) = [Ax], \ \ \forall \ A \in GL(m + 1, \mathbb{R}) \ , \ \forall \ x \in \mathbb{R}^{m+1}.$$

Therefore, in particular, rather than considering projective shapes of configurations in $\mathbb{R}^3$, we consider projective shapes of configurations in the projective space $\mathbb{R}P^3$.

5 Age depending projective shape anti-regression in Acrosterigma Magnum shells

Our data consists of digital camera images of a species of clam shells collected from the Florida coast of the Gulf of Mexico. We use *Agisoft* to reconstruct the 3D the surface

of the shells, and as a side advantage we obtain the 3D coordinates of a conveniently selected group of landmarks. These are used in performing a landmark based 3D projective shape anti-regression analysis.

5.1 Landmark data collection

For the data collection part, at this point we have collected 33 shells from the Acrosterigma Magum species. All the shells are numbered by their size from the largest to the smallest. We counted the ridges on the shells that are due to seasonal changes in the shells growth, thus reflecting their age (e.g. shell No.1 is 80 yrs old, shell No.2 is 120 yrs old, etc.). The age is the predictor variable. The projective shape of the group of landmarks is the response variable. Also, size could be used as predictor variable, however it does not necessarily reflect the age of a shell.

To capture the main feature of the shell shape, we marked on the shell surface seven corresponding landmarks as follows: two points are on the first and third quarter shell ridge, and three points are selected on the middle ridge. On each ridge, the points were selected as one quarter, half and three quarter distance from the ridge length. This landmark insures an accurate marked correspondence, that is also age consistent (see Figure 1).

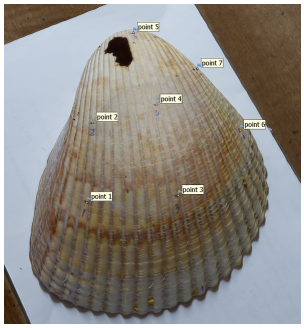

Figure 1: Landmarks placements for shell No.1

After marking all the shells, we took for each shell between 15 and 25 photos, and imported the images to Agisoft. By using this software, it was easy to extract the 3D coordinates for each landmark, by conducting a few work-flows (see Figure 2).

Table 1: 3D coordinates of shell 1

	x	y	z
point1	-0.06755	0.004022	0
point2	0.036703	0.959274	-1E-06
point3	1.030844	0.036704	0.000002
point4	0.816805	1.131873	0.083043
point5	0.566299	2.185978	-0.53225
point6	1.87667	0.870082	-0.62797
point7	1.366106	1.673462	-0.52259

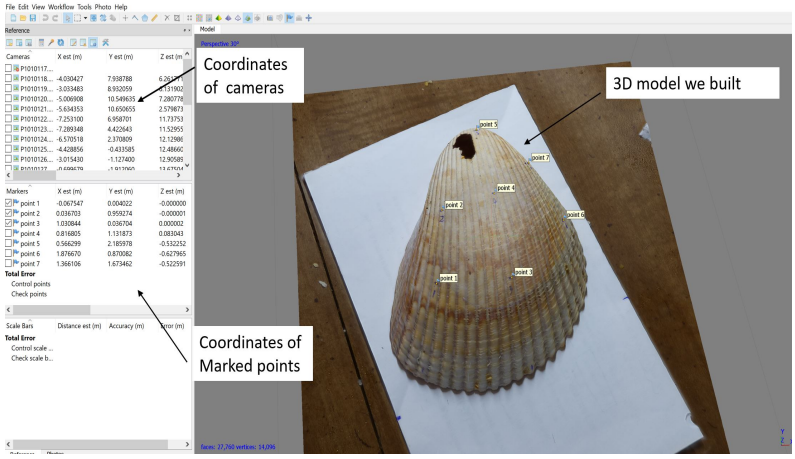

Figure 2: The Agisoft window displaying 3D coordinates

5.2 Projective shape reconstruction

Let us assume that $x_1, \ldots, x_{m+2}$ are points in general position and let $x = (x^1, \ldots, x^m)$ be an arbitrary point in $\mathbb{R}^m$. In this notation the projective coordinate of x with respect to the projective frame associated with the $m+2$ points $x_1, \ldots, x_{m+2}$ is the same as the projective coordinate of $p = [x^1 : \cdots : x^m : 1]$ with respect to $(p_1, \ldots, p_{m+2})$, where $p_a = [x_a^1 : \cdots : x_a^m : 1]$ (for a definition of projective coordinates see (4.2)). The projective coordinate of the point x (see Mardia and Patrangenaru(2005)[6]) is given by

$$[z^1(x) : z^2(x) : \cdots : z^{m+1}(x)], \tag{5.1}$$

where

$$\begin{aligned} & z^j(x) = y^j(x)/||y(x)||, j = 1, \ldots, m+1, \\ & y^j(x) = v^j(x)/v^j(x_{m+2}), \\ & y(x)^T = (y^1(x), \ldots, y^{m+1}(x)), \\ & z(x) = (z^1(x), \ldots, z^{m+1}(x))^T, ||z(x)||^2 = 1, \\ & v(x) = (v_1(x), \ldots, v_{m+1}(x))^T = U^{-1}p(x) \end{aligned} \tag{5.2}$$

with the $(m+1) \times (m+1)$ matrix

$$U = [p(x_1), \ldots, p(x_{m+1})], \tag{5.3}$$

where $p(x) = (x^T, 1)^T$.

In our case $m = 3$, therefore we select the first $m + 2 = 5$ points as the projective frame. By the algorithm above, we can calculate the projective shapes for our data as $z_i, i = 1, \ldots, 33$, where in spherical representation, $z_i \in \mathbb{S}^3 \times \mathbb{S}^3$. For example, the projective coordinates representation for the first shape for the first shell is:

$$z_1 = ([z_1^1], [z_1^2]) = \begin{pmatrix} 0.4705 & 0.4979 \\ 0.4143 & 0.4544 \\ 0.6030 & 0.5609 \\ 0.4934 & 0.4808 \end{pmatrix},$$

where

$$z_1^1 = (z^1(y_6), \ldots, z^4(y_6))^T = (0.4705, 0.4143, 0.6030, 0.4934)^T,$$
$$z_1^2 = (z^1(y_7), \ldots, z^4(y_7))^T = (0.4979, 0.4544, 0.5609, 0.4808,)^T.$$

5.3 *VW*-anti-regression results based on age

We use age as independent variable and projective shape as dependent variable. After applying our nonparametric anti-regression model, the relationship between the estimated marginal VW-antimean projective shape, as a function of age is shown in Figure 3.

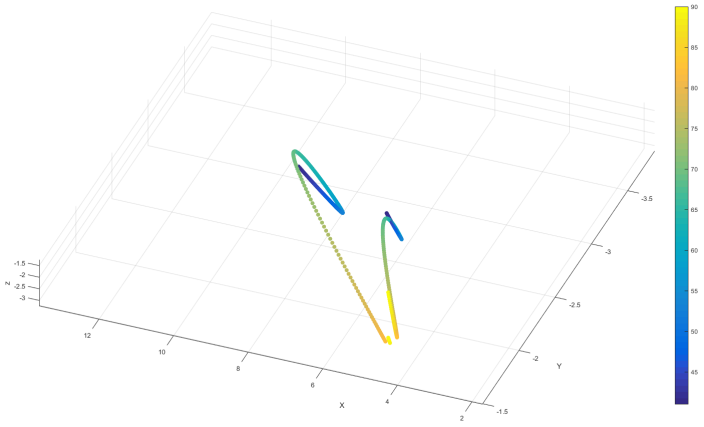

Figure 3: Marginal distribution of the antimean projective shape of the 7-ad, in the affine coordinate representation of the two projective coordinates

From the two curves in Figure 3, it is easy to see the antimeans are relatively stable around 40 years old and 90 years old shells. Note that the changing rate of the antimean projective shapes is larger somewhere in the middle of the lifespan than at the two ends of these two age depending curves.

6 Discussion

Two important anti-regression methods could be employed, the *extrinsic* method, using an embedding and the *intrinsic* method, using a Riemannian metric. The intrinsic method is based on a geodesic distance, which is time consuming to compute;

moreover no explicit formula for the intrinsic antimean is known yet. The main problem with intrinsic antimean, is that there is no necessary condition for its existence (same as with intrinsic means). In general, compared with the intrinsic method, the *extrinsic* method is computationally more efficient and practical to use (see [1]).

Manifold valued data may be spread all over the compact object space. For this reason, while extrinsic mean analysis is a good method to capture the data location, when it is not too spread, it may not suffice to represent the location of the data in general. This is our motivation to suggest the anti-regression method.

In this paper, we applied *VW*-anti-regression analysis for projective shapes of selected landmark configuration on the shell surface, which seems to point out that the antimean shape is much more stable around two ends of the age predictor than during their mid-life. It is reasonable to believe that the suggested anti-regression method can be applied to a variety of object data to explore hidden features, thus the anti-regression is worth pursuing further.

References

[1] R. N. Bhattacharya, L. Ellingson, X. Liu, V. Patrangenaru and M. Crane, *Extrinsic analysis on manifolds is computationally faster than intrinsic analysis, with applications to quality control by machine vision*, Applied Stochastic Models in Business and Industry **28** (2012), 222–235.

[2] M. Crane and V. Patrangenaru, *Random change on a Lie group and mean glaucomatous projective shape change detection from stereo pair image*, Journal of Multivariate Analysis **102** (2011), 225–237.

[3] M. Fréchet, *Les élements aléatoires de nature quelconque dans un espace distancié*, Ann. Inst. H. Poincaré **10** (1948), 215–310.

[4] Kendall, D. G., *Shape manifolds, procrustean metrics, and complex projective spaces*, Bull. London Math. Soc. **16**, (1984), 81–121.

[5] Kanti V. Mardia and Peter E. Jupp, *Directional statistics*, John Wiley & Sons, Ltd., Chichester, 2000.

[6] K. V. Mardia and V. Patrangenaru, *Directions and projective shapes*, Annals of Statistics **33** (2005), 1666–1699.

[7] V. Patrangenaru, *New large sample and bootstrap methods on shape spaces in high level analysis of natural images*, Commun. Statist. **30** (2001), 1675–1693.

[8] V. Patrangenaru and L. Ellingson, *Nonparametric Statistics on Manifolds and Their Applications to Object Data Analysis*, CRC-Chapman & Hall, 2015.

[9] V. Patrangenaru, X. Liu and S. Sugathadasa, *Nonparametric 3D projective shape estimation from pairs of 2D images - I, In memory of W.P. Dayawansa*, Journal of Multivariate Analysis **101** (2010), 11–31.

[10] V. Patrangenaru and K. V. Mardia, *Affine shape analysis and image analysis*, Proceedings of the Leeds Annual Statistics Research Workshop 2003, 57–62.

[11] V. Patrangenaru, K.D.Yao and R. Guo, *Extrinsic means and antimeans*, In: Cao R., González Manteiga W., Romo J. (Eds), "Nonparametric Statistics", Springer Proceedings in Mathematics & Statistics, **175** (2016), 161–178.

[12] Patrangenaru, Vic and Guo, Ruite and Yao, K. David, *Nonparametric inference for location parameters via Fréchet functions*, Second International Symposium on Stochastic Models in Reliability Engineering, Life Science & Operations Management 2016, 254–262.

[13] H. L. Resnikoff, *Differential geometry and color perception*, J. Math. Biol. **1**, 2, (1974/75), 97–131.

Authors' addresses:

Yifang Deng and Vic Pătrăngenaru
Florida State University, Tallahassee, FL, USA.
E-mail: vic@stat.fsu.edu , yd14d@my.fsu.edu

Vladimir Balan
University Politehnica of Bucharest, Romania.
E-mail: vladimir.balan@upb.ro